Tutor/s

Dr. Jordi Ignés Mullol
Departament de Ciència de Materials i Química Física

Grau de Química

Treball Final de Grau

Fabrication of Colloidal Materials through Microfluidic Techniques.

Fabricació de Materials Col·loidals mitjançant Tècniques de Microfluídica.

Joel Torres Andrés

June 2022

Universitat de Barcelona

B:KC Barcelona Knowledge Campus
Campus d'Excel·lència Internacional

Well, I didn't know it was hard.

Ivan Sutherland, 1987.

Primerament, voldria agrair la presència de la meva família i amics. També fer menció especial als integrants del laboratori 4017 i al Jordi pels seus consells i paciència. A totes elles, gràcies per participar d'alguna forma en aquestes pàgines i aguantar a la *drama-queen* que ha elaborat aquest escrit.

REPORT

IDENTIFICATION AND REFLECTION ON THE SUSTAINABLE DEVELOPMENT GOALS (SDG)

The field of microfluidics has shown its potential as a new way to perform analysis and synthesis of new materials, reducing the number of reagents needed and thus, being a greener alternative to conventional methods. Regarding the synthesis of new materials, this new scientific field, and especially drop generation techniques, provide a new insight in terms of developing innovative solutions based on exploring the chemistry at a micro or even nanoscale.

In this report, polymer spheres are generated through a needle-based drop-generator system, and these are coated with a silica shell which provides the material with wide surface functionalization capabilities. In fact, is this capability of modifying surface properties that puts an eye on the material, regarding to possible applications it can have. In these pages, it is shown that a silica shell is generated in no more than 24 hours and a coating procedure to make the surface hydrophobic is accomplished within 30 min.

In terms of applications to promote the accomplishment of the Sustainable Development Goals, spheres with properly tunned surface properties can be used in the field of water purification, which can be associated with goals 6 (Group 1-People's Wellbeing), Safe Water and Sanitation, and 14 (Group 3- Planet Earth's Conservation), Life Below Water, because of the material's potential capacity of removing water pollutants[28].

Binding the proper molecule to the surface provides the spheres with the capability of removing metal cations from water, if the molecule attached to the surface is a chelator agent or if the molecule is charged, acting as an ion exchange system. Further from this, interaction tuning through surface functionalization, can be applied to capture other type of pollutants.

Therefore, as stated before, this cleaning capacity of the surface-modified spheres goes with goal 14, (which consists of conserving and using sustainably the oceans, seas, and marine resources), and especially the objective 14.1, stating the necessity of reducing and preventing the contamination of waters. This pollutant removal activity can be related to goal 6 as well (which is focused on guaranteeing water availability and its sustainable management and sanitation for everyone), and within this, point 6.3, which exposes the necessity of reducing water contamination, where functionalized spheres can provide new approaches to solve the issue[28].

CONTENTS

1. SUMMARY

Microfluidics is the science and technology of fluid manipulation on the microscale through the creation of fluidic systems with a channel width of less than 500 μm. Since its appearance during the second half of the XXth century, this relatively young field has gained attention due to the properties arising because of the channel size reduction, such as the disappearance of turbulent flows.

Among the wide range of microfluidics applications, the creation of monodisperse colloidal systems is one of the most promising branches of this science. With the use of drop-generator microfluidic devices, stable monodisperse emulsions can be created, where each drop can behave as an independent micro-scale reactor, providing new possibilities in the research fields of chemical and biological analysis as well as new materials development.

The main material used to build the devices is glass. Glass is stable and highly manipulable from a chemical and physical point of view. However, its manipulation to create the devices sometimes can lead to complex and risky operations. Therefore, the exploration of new easy-to-make and inexpensive procedures is necessary to approach microfluidics in an out-of-the-lab environment.

In this report, the creation of drop-generator microfluidic devices based on dispensable needles will be assessed, comparing their building procedure and performance to the ones observed in the case of glass-based devices. Furthermore, with the use of needle-based devices, functional colloidal systems based on polymer spheres are created as a practical application of the developed technique.

Keywords: Microfluidics, monodisperse colloidal systems, functional polymer spheres.

2. RESUM

La microfluídica és la ciència i la tecnologia de la manipulació a escala microscòpica dels fluids mitjançant la creació de sistemes de fluídica amb canals de circulació de gruixàries inferiors als 500 μm. Des de la seva aparició durant la segona meitat del segle XX, aquest camp s'ha guanyat l'atenció del món científic gràcies a les noves propietats que presenta a raó de la reducció de la mida dels canals de circulació.

Dins del rang d'aplicacions de la microfluídica, la creació de sistemes col·loidals monodispersos representa una de les branques més prometedores. Amb l´ús de dispositius generadors de gotes, es poden crear emulsions monodisperses i estables, on cada gota que conforma el sistema, pot actuar com un microreactor independent, aportant, doncs, oportunitats pel desenvolupament de nous mètodes als camps de l'anàlisi i la síntesi de materials.

El material principal usat en la construcció d'aquests dispositius és el vidre. El vidre és estable i fàcilment modificable des del punt de vista químic i físic. No obstant, la seva manipulació a l'hora de crear els dispositius poden involucrar operacions complexes, cares i amb un cert risc associat. És per això, que cal explorar nous mètodes de construcció barats i fàcils per apropar el món de la microfluídica a un àmbit fora dels laboratoris d'investigació.

A aquest treball, s'exposa la creació de dispositius generadors de gotes basats en agulles d'un sol ús, comparant el procediment de muntatge i la seva capacitat per a generar emulsions monodisperses amb els dispositius construïts a base de capil·lars de vidre. A més, a través dels dispositius d'agulles, es fabricaran sistemes col·loidals funcionals basats en esferes polimèriques com a possible aplicació de la tècnica desenvolupada.

Paraules clau: Microfluídica, sistemes col·loidals monodispersos, esferes polimèriques funcionals.

3. INTRODUCTION

Microfluidics is the science and technology of fluid manipulation on the microscale through the creation and monitorization of systems with integrated channels with a width of less than 500 μm[1]. So, it can be regarded as the miniaturization of fluidic systems from the macro-scale to the micro-scale.

The main purpose of microfluidics is the creation of lab-on-a-chip systems which offer a new era in terms of sample analysis, new material synthesis and engineering, thanks to the small volumes of reagents and samples used, less analysis or reaction time and the high reproducibility shown by these chips[2,3]. In addition to this, the miniaturization to the micro-scale of the fluidic systems (pipes, valves, etc.) and thus, the fluids' volumes, generates the surging of new behaviour, which is not seen on the macroscale, mainly due to an increase in the specific surface of the fluids circulating through the system. These new arising characteristics are related to three main phenomena[4]: highly efficient mass-heat transfer, significant surface effects and viscous forces predominating over inertial forces.

Since its arising during the second half of the XXth century, due to the necessity of developing new detecting systems based on fluid manipulation on the micro-scale to improve already existent techniques, such as gas or liquid chromatography, in terms of sensitivity and resolution by only using small sample quantities[2], microfluidics has experienced significant growth in the field of physical and life sciences, as this discipline offers a wide range of possibilities in terms of analysis, reactivity and processing[1–4]. Among these developments, drop generation, which will be discussed in this report, is one of the most promising branches of this field, as it allows the creation of small and reproducible miniaturized chemical systems.

3.1. LAMINAR FLOW

As a result of the miniaturization, the shrunk systems are provided with new characteristic behaviour which is not present in their macro-sized analogues[1]. One of the most important features that appear with a decrease in the size of the system's canalizations is that inertial forces, forces that describe the resistance of the liquid volume to change its flow velocity,

become insignificant compared to the ones generated by the viscosity of the fluid, forces which are intrinsic to the liquid and appear because of the intermolecular interactions. This predominance of viscosity over inertia in the different fluxes generates the elimination of turbulent flows, meaning that when two different fluids come in contact inside a microchannel, they do not mix convectively, they circulate parallelly through the channels without eddies or turbulence, a state known as laminar flow[4]. The relation between inertial and viscous forces is described by Reynolds number (Re), a dimensionless parameter. Equation I shows the description of the Reynolds number[3].

$$\mathrm{Re} = \frac{\rho u L}{\eta} \qquad \text{Eq. I}$$

Where ρ is the density of the fluid, u is flow mean speed in m/s, η is the dynamic viscosity of the circulating fluid and L is the characteristic length, which, in these systems, is regarded as the inner diameter of the channels[3].

Looking carefully at the parameters involved in the characterization of Re, L and u play a vital role in determining the predominance of viscous forces. The micro-sized channels and the low volume employed in these systems lead to low Re values, demonstrating the predominance of viscosity over inertia in the description of the laminar fluxes' behaviour[3,4].

Within a laminar flow regime, the only mixing occurring between different fluids flowing parallelly inside a microchannel is due to molecular diffusion through the interface of the two fluids[4]. Molecular diffusion is a slow process, which means that on a small time scale, mixing between two fluxes in contact is not appreciated. According to this, and the fact that no eddies and turbulence are observed, laminar flow is crucial when drop formation comes, because it generates a stable flow system where no distortions could lead to drop splitting through surface deformations caused by fluids' fluctuations.

3.2. COLLOIDAL SYSTEMS GENERATED THROUGH DROP-GENERATOR MICROFLUIDIC DEVICES

Within microfluidics, drop generation is one of the most promising branches of this science. Drop generation through microfluidic systems consists of the creation and manipulation of discrete drops embedded in a continuous fluid phase inside microchannels[1,2]. The continuous fluid phase and the fluid phase which originates the drops are immiscible.

These devices generate a highly monodispersed set of individual drops which can be manipulated independently. In addition to this, the composition of both fluid phases can be adjusted precisely to generate the desired properties. Thanks to this, drop generation principal motivation is focused on biological and chemical analysis and synthetic methods for new materials, as each drop can behave as an independent micro-reactor[1,4].

The systems created through drop generation microfluidic devices are understood from a chemical point of view as an emulsion[5]. Emulsions are colloidal systems (systems and materials with characteristic lengths comprehended between 1 nm and 10 μm) made of a biphasic system of two or more liquids in which at least one of them is dispersed into drops embedded in the others. The liquids that compose the drops (dispersed phase) need to be immiscible or poorly soluble with the liquids in which the drops are dispersed (continuous phase).

The necessity of high energy inputs to create emulsions comes from the high contact surface between the two phases (due to the small and numerous drops composing the system) and the overpressure experienced by the drops because of the curved interphase between the two liquids, which increases when the radii of the drops decrease. Both factors mentioned are directly related to the cohesive forces (the tendency of the molecules to stay together) and non-favourable interaction between the phases[6]. To reduce the free energy of the system, the dispersed phase acquires the shape of a sphere, which has the smallest area per volume ratio, leading to a configuration with the least interphase.

This energy supply in microfluidics can come from an inner source such as the continuous phase in which the drops are embedded, or an external source. Depending on the origin of the energy required to drop formation two drop generation methods arise[4]. If the energy supply comes from an external force applied to the system (for example an electric or a magnetic field) the generation method is regarded as active, whereas, if the energy required for drop generation occurs via surface instabilities induced by continuous phase flow profiles, the method is classified as passive. In this report, drop generation will occur through passive methods[3].

In addition to this, to reduce the amount of energy needed to create emulsions and make them relatively durable, chemical species are introduced into the system to generate kinetic stability (to induce metastability) to the system, as well as a reduction in the interaction energy between the immiscible phases[6]. These species can be solids, hydrocolloids, or surfactants.

Ideally, the species added need to reduce the surface tension (γ-described as the energy per surface area needed to increase the interphase) below 10 Nm^{-1}, provide charge to the drops on the surface, have rapid adsorption, and be effective at low concentrations or increase the viscosity of the continuous phase.

Interesting facts for this project are that polydisperse emulsions (emulsions with a high range of drop sizes) are more unstable than monodisperse drop systems. This is due to Ostwald Ripening, which explains that, in a polydisperse system, smaller drops have higher overpressures due to a higher curvature of their interphase and so the molecules that compose the drops tend to diffuse to bigger drops to reduce the total contact surface and thus, reduce the energy of the whole system[7].

3.2.1. The devices

Microfluidic devices consist of three main parts[2]: Channels through which fluids circulate, the pump system and the main body where the function of the device is performed. In the case of a passive drop-generator, the main body consists of a junction of channels where the two immiscible phases meet. Depending on the configuration of the junction, different systems of drop formation appear[3,4]. An image of each device's disposure is seen in figure 1.

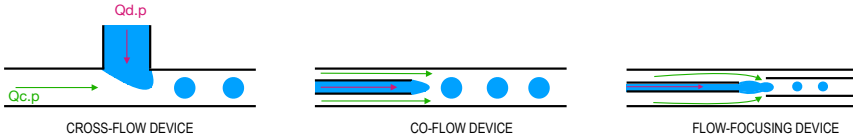

Figure 1. Different types of devices as a function of the systems' distribution ($Q_{c.p}$ stands for continuous phase flow and $Q_{d.p}$, for dispersed phase flow).

In this work, only flow-focusing will be used. In flow-focusing, the system's shear is enhanced because of the incorporation of a collecting microchannel coaxial to the inner inlet channel and thus, it is easier to reach stable conditions where a monodisperse drop formation regime occurs.

The construction parameters of the device influence the drops' size distribution[3,4,8,9]. Those parameters are the diameters of the used tips and the distance between the tips. It has been noticed that when the distance between the inner microchannels working as inlets and outlets is reduced, shear-focusing is enhanced and smaller drops are obtained[8,9].

Coatings and surface manipulation can be performed to regulate the wettability of the different liquid phases and produce W/O or O/W[8,10] emulsions. Consequently, there, surface conditions play an important role in the type of emulsion being produced. Generally, the surfaces of the microchannel should match the nature of the continuous phase used (whether the liquid is hydrophilic or not).

The materials used to construct the devices range from polymer to glass, with 3D o 2D spatial distributions. All the different materials present benefits and drawbacks from an economical and manipulation point of view. For example, glass-based devices show high structural stability optical transparency and chemical inertness but involve difficult building procedures and risks derived from manipulation of sharp tips, and can be expensive, depending on the overall system[1,2].

3.2.2. Forces

As well as the architecture of the device, the control in the drop formation also depends on the parameters which characterize both immiscible phases, in terms of composition, interaction and flow.

The first parameter to be considered to analyse the passive drop formation is the Weber number[3,4] (We), a dimensionless parameter which describes the inertial to interfacial forces ratio. The equation related to We can be seen in equation II[9].

$$\mathrm{We} = \frac{16\rho u^2}{\pi^2 \gamma \emptyset^3} \qquad \text{Eq. II}$$

Where ρ is the density of the dispersed phase, u flux velocity in m/s of the dispersed phase, ø is the diameter of the drop and γ is the surface tension between the two immiscible phases.

Depending on whether the inertial forces or the surface forces predominate, two drop formation main regimes can be observed[3,9] in figure 2.

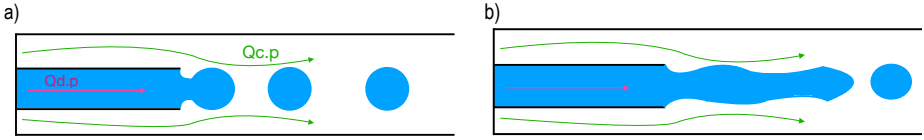

Figure 2. Drop generation regimes, dripping (a), and jet formation (b).

The transition between the two regimes is principally based on the flux flow of the continuous phase during the performance of the experiments, since neither the diameter of the drops (which at the end is controlled by the construction parameters of the device), the surface tension between the two immiscible phases or the density of the fluid can be changed while the setup is working[8].

The required conditions to acquire a highly monodisperse drop formation system is when a dripping regime is observed[9], so the flux of the continuous phase needs to be low enough just to make the surface interaction forces overcome the inertial forces derived from the fluid's flux[4].

Another parameter which needs to be considered when working with drop formation microfluidic devices is the capillary number (Ca) which describes the viscous to interfacial forces ratio. The description of this ratio can be seen in equation III[3].

$$\mathrm{Ca} = \frac{u\eta}{\gamma} \qquad \text{Eq. III}$$

Where η represents the dynamic viscosity of the phase (usually the continuous phase), u represents the flow velocity and γ represents the surface tension.

The breaking up of the dispersed phase into small drops is due to the presence of surface instabilities and the continuous phase flow profile just at the point where the drops are formed. The main factor which provokes the splitting of the dispersed phase is the shear induced by continuous phase arising from its viscosity[3,4,9].

If slow shear is present, there is not enough force to produce surface instabilities and split the dispersed phase into drops, and because of working at a low Reynolds number, no mixing between the two immiscible phases will occur. Therefore, a shear which is competitive with the surface interactions needs to be present if drops smaller or comparable to the size of the dripping tip want to be produced. This happens because vicious forces start to predominate and become competitive towards interfacial forces, provoking splitting through surface instabilities.

In general words, Ca controls the size of the drops. An increase in Ca provokes a lowering in the size of the drops formed, which means that the viscous forces start to become competitive with the interfacial forces[8]. In most cases, Ca numbers[4] are between 10^{-2} and 10^{-4}. As Ca has flux velocity involved in its formulation, in the case of the dispersed phase, if high Ca numbers are present, a jet regime could be achieved[3].

4. OBJECTIVES

The aims of this experimental work can be divided into two main parts:

1. Explore two possibilities of creating a drop-generator microfluidic device based on dispensable needles and plastic structures and compare them with glass-based devices in terms of performance and building procedure, all oriented towards a future application in an academic lab course. In Chapter 5, the behaviour of the needle-based devices is assessed and compared with the performance of glass-based devices.

2. Generate polymer spheres through the built needle-based devices and explore further surface functionalization. In Chapter 6, ETPTA polymer spheres' creation will be studied, as well as the capability of these to form colloidal crystals. Furthermore, ETPTA spheres' surface modification will be carried out through the functionalization of a silica shell disposed over them.

5. DROP-GENERATOR MICROFLUIDIC DEVICES

5.1. BEHAVIOUR OF NEEDLE-BASED DEVICES

5.1.1. Non-functionalised devices

With the use of devices **I**, **II** and **III** (see section 7.2.2.1) drops are generated with different flow rates using a 2% wt. aqueous solution of surfactant F-127 as the continuous phase and hexadecane oil as the dispersed phase[8]. The results in terms of drop generation performance can be seen in figure 3.

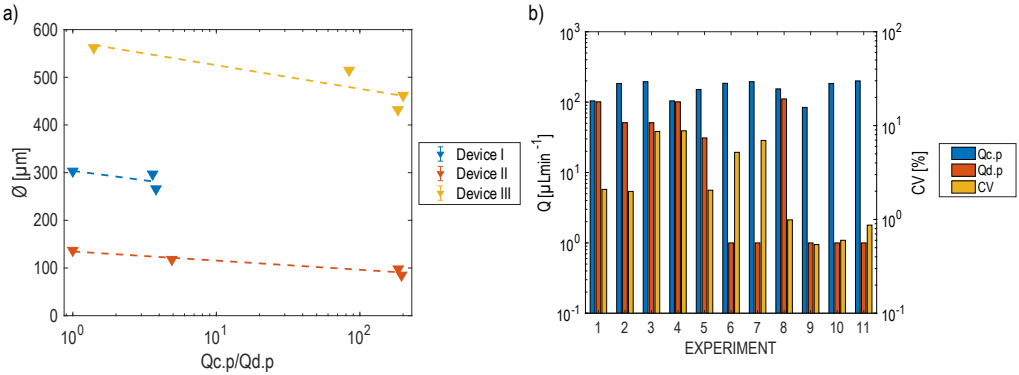

Figure 3. Results for 30G+34G devices and 22G+27G device in hexadecane drops formation. In (a) is shown the drop diameter (Ø) as a function of the flow ratio (where $Q_{c.p}$ is the continuous phase flow rate and $Q_{d.p}$ is the dispersed phase flow rate). Plotted lines are guides for the eye. In (b) a bar diagram of polydispersity (CV) and flow rates of the phases is seen. Experiments 1, 2 and 3 are related to device I, experiments 4, 5, 6 and 7, to device II and 8, 9, 10 and 11 to device III.

The first remarkable thing seen in figure 3 (a), is that a determinant factor of the drop size is the architecture of the device. It is observed that the diameter of the drops is strongly related to the diameter size of the needles used. When the diameter of the used needles is increased, the drop size also increases. This is highly noticed if a comparison between the diameters obtained through the 22G+27G device (**III**) and 30G+34G devices (**I** and **II**) is made. Moreover, the inter-needle tips distance also plays an important role in determining drops' size, as noticed by comparing the drop size acquired with the 30G+34G devices (**I** and **II**). Closer tips are related to smaller drops and the size of these reassemble the inner diameter of the dispersed phase inlet needle, whereas higher distances generate bigger drops with a size much similar to the collecting needle. This evidence is consistent with the fact that the strongest shear forces occur at the tip of the collecting needle, where flow-focusing occurs, meaning that the further the dispersed phase inlet is from the outlet, the smaller the shear force is, generating the necessity of larger drop surfaces to provoke instabilities and so, to promote splitting (which means bigger drops)[3].

In addition to this, when performing drop generation, in every case independently of the devices' architectures, it is shown that when a larger $Q_{c.p}/Q_{d.p}$ ratio is present the diameters of the drops decrease[3]. This is closely related to Ca. An increase in the $Q_{c.p}$ generates higher flow

velocities of the continuous phase, as the diameters of the microchannels are maintained. Therefore, this increase in the flow rate leads to a larger Ca number, generating a stronger presence of viscous forces (an increase in the shear at the dripping tip which helps to drop splitting in a dripping regime thanks to the generation of bigger surface instabilities).

Figure 3 (b) shows that higher values of $Q_{c.p}$ and $Q_{d.p}$ for each device, generally generate higher values of polydispersity, although there is a lot of dispersion. This is because higher $Q_{c.p}$ values generate stronger shear forces and thus, higher surface instabilities, promoting non-regular drop splitting. In the case of $Q_{d.p}$, higher values of this parameter provoke a stronger influence of inertial forces (an increase in We) that leads to the destabilization of the dripping regime towards a jet formation, which generates polydisperse drops.

5.1.2. Functionalised devices

Experiments performed with a needle surface functionalization with OTS (device **IV-**see section 7.2.2.2) allow the formation of W/O dispersions consisting of 2% wt. mixture of surfactant F-127 in water as the dispersed phase and hexadecane oil as the continuous phase (figure 4).

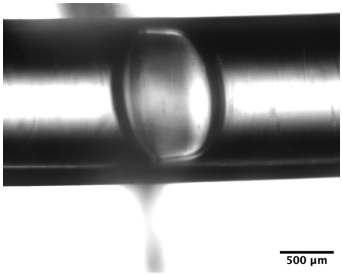

Figure 4. Water drop dispersed in hexadecane oil inside the collecting tub.

This shows the connection between the hydrophobicity of the surfaces with the emulsion type that wants to be created. A proper outlet needle functionalization is required to maintain the stability of the system along with its collection. As the generated drops are going to be close to the surface inside the outlet needle, if the surface interactions between the dispersed phase and the needle are more favourable than the one between liquid phases, drops will attach to the surface and generate a phase separation between both liquids involved. Accordingly, surface functionalization should be considered to match the hydrophobicity of the continuous phase[10]. With this, a layer of continuous phase will be created between the surfaces and the drops, providing stability to the system.

5.2. GLASS-BASED AND NEEDLE-BASED DEVICES IN ETPTA DROPS FORMATION

5.2.1. Drops generated through needle-based devices

Having the photoinitiator HMPP (1.39 % wt.) in reticulated hydrophobic monomer ETPTA as the dispersed phase and 2% wt. an aqueous solution of surfactant F-127 as the continuous phase, drops are created with the use of devices **I** and **II**. The results in terms of drop generation performance can be seen in figure 5.

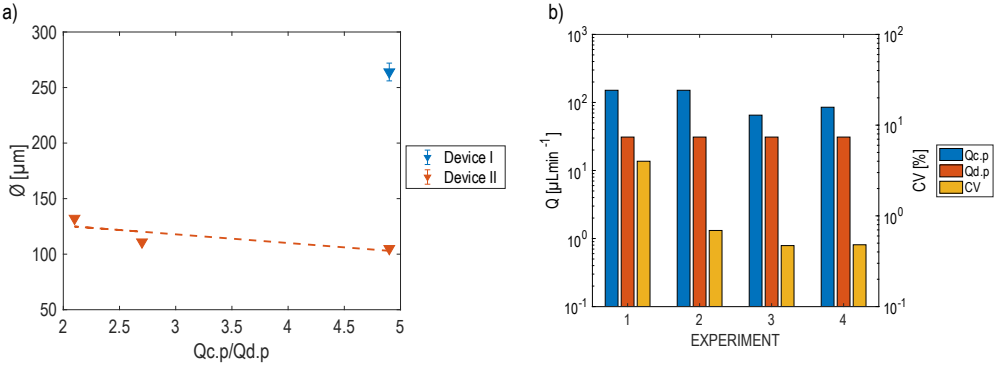

Figure 5. Results for ETPTA with HMPP drop formation in 30G+34G devices. In (a) is shown the drop diameter (Ø) as a function of the flow ratio (where $Q_{c.p}$ is the continuous phase flow rate and $Q_{d.p}$ is the dispersed phase flow rate). Plotted lines are guides for the eye. In (b) a bar diagram of polydispersity (CV) and flow rates of the phases is seen. Experiments 1 is related to device I, and experiments 2, 3 and 4, are to device II.

The same tendencies seen when performing similar experiments with hexadecane oil as the dispersed phase are observed. Higher $Q_{c.p}/Q_{d.p}$ values induce lower values for the size of the drops. Also, higher flow rates of both phases induce higher values of polydispersity. In addition to this, it is also observed that lower inter-needle tips distances, lead to a lowering in the drops' size. However, as the dispersed phase has changed compared to the previous experiments, one must consider that the parameters (We and Ca) that regulate drop generation have changed in terms of the values related to intrinsic characteristics of the phase, such as viscosity.

5.2.2. Drops generated through glass-based devices

Using device **V** (see section 7.2.3), drop formation is performed with the photoinitiator HMPP (1.39 % wt.) in the reticulated hydrophobic monomer ETPTA as the dispersed phase and 2% wt. aqueous solution of F-127 as the continuous phase[8]. The results are shown in table I.

Experiment	$Q_{c.p}$ [μLmin^{-1}]	$Q_{d.p}$ [μLmin^{-1}]	$Q_{c.p}/Q_{d.p}$	Ø [μm]	CV [%]
1	155.1	1.0	155.1	44.8 ± 0.5	2.33
2	155.1	11.0	14.1	JET	-
3	185.1	21.0	8.81	JET	-

Table I. Results for glass-based device.

The drops generated by a glass device are smaller and more numerous than the ones created through a needle-based device. As seen in figure 5 and compared to table I, the drops are smaller and with a slightly bigger polydispersity.

Higher values of $Q_{d.p}$ lead to the formation of a jet of the dispersed phase, as seen in experiments 2 and 3. The appearance of a jet regime leads to a non-favourable condition to generate monodispersity[4]. In figure 6 it is seen a jet formed when conditions in experiment 2 were present. The jet formation is explained based on two main aspects: high inertial forces related to the dispersed phase and low shear values to provoke drop splitting just where the two different phases met.

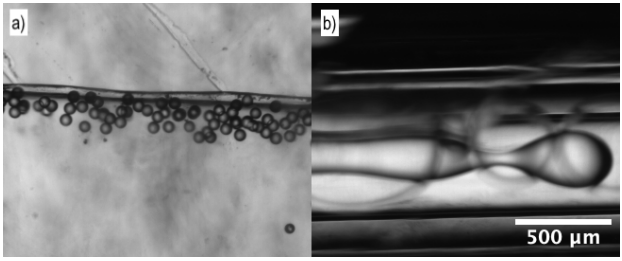

Figure 6. (a) ETPTA drops created through a glass-based device using the flow rates of experiment 1 of Table I and (b), ETPTA jet formed under the conditions exposed in experiment 2 of Table I.

Since the sizes of the pulled tips of the inner capillaries are smaller than the ones of needles, smaller drops can be created. Thanks to the tip-pulling technique and microforging (see section 7.2.3) is relatively easy to cut the tips at the selected diameters, leading to a wide range of possibilities in terms of device architecture to apply flow-focusing.

5.2.3. Comparison

Glass-based devices have a more stable structure than needle-based devices. Thanks to the capillary pulling technique and microforge, is relatively easy to construct devices with highly controlled tip sizes. Both factors contribute to the fact that smaller, highly monodisperse drops can be generated at high rates. The capability of reaching higher pressures than the needle-based devices, makes glass capillary devices ideal for working at high flow rates, which require higher pressures coming from the pump. In addition to this, needle-based devices are more opaque to light than glass-based ones. This means that the utile life (life until polymerization occurs via ambient light) of glass devices when generating photopolymerizable droplets is smaller, requiring more strict illumination control conditions when performing the experiments.

In terms of construction time, needle-based devices show the shortest building time as the protocol involved in their construction does not involve techniques such as microforging, which require some skill and practice before reaching the desired results. In addition to this, surface cleaning and system preparation is easier when employing needles. Moreover, the sharp tips involved in glass-based devices, contrary to the blunt needles used in needle-based devices, represent an additional risk to consider when deciding whether to develop an experimental procedure for an out-of-research environment. However, glass devices are mainly constructed with recyclable materials (they are composed of glass) reducing the impact on the environment. Contrarily, needle-based devices have single-use plastic parts in their structure (needle adaptors, T-junction, …) which are not considered environmental-friendly materials but, some exploration can be done to replace and reuse single-use plastic materials in needle-based devices, and metallic parts from the needles could be separated from plastic to improve its recyclability.

So, considering all, needle-based devices show a great opportunity to replace glass-based devices. As an extension of this analysis, these easy-to-build systems which reduce time and risks of manipulation could end in an interesting academic approach to studying emulsions and microfluidics in master's or degree's lab practices. As microfluidics is a promising field within chemistry, introducing easy to perform experimental procedures into a students' practicum program is interesting in terms of presenting a new world for exploration which can increase motivation and curiosity. Moreover, these devices could lead to further experimental setups and the development of new applications for the academia.

6. FUNCTIONAL COLLOIDAL MATERIALS GENERATED THROUGH MICROFLUIDICS

6.1. POLYMER SPHERES

6.1.1. Drop polymerization

Once formed, the drops are polymerized through two alternative procedures. The first procedure consists of polymerizing the drops with UV light once collected from the device. The other procedure, in-flow polymerization, is based on applying UV light while the drops are circulating through the channels (see section 7.4.1). Better results in terms of monodispersity were obtained with an in-flow polymerization (figure 7). This procedure ensures the maintenance of the shape and size of the drops thanks to preventing coalescence at the collecting zone due to drop accumulation.

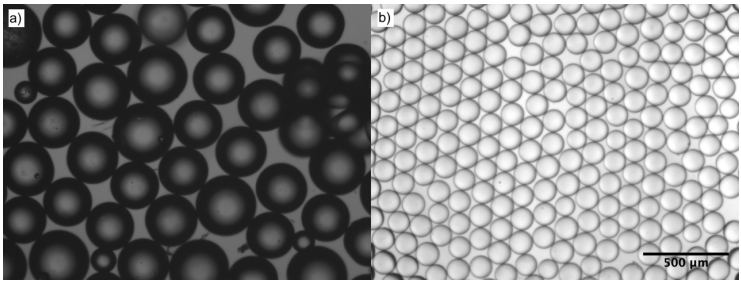

Figure 7. Polymer spheres obtained through (a) after-collecting polymerization and, (b), through in-flow polymerization.

To characterize and demonstrate that the polymerization has occurred, continuous phase evaporation of two emulsions created using the same conditions was performed (figure 8). Both emulsions (only one of them, irradiated with UV light after collecting) were deposited over a glass slide and heated at 50ºC until dryness, recording images of the process every 30 seconds.

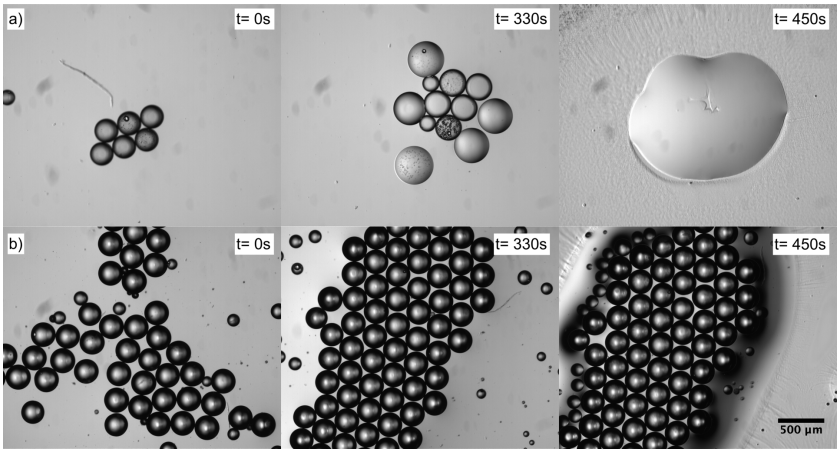

Figure 8. Drying procedure at different times of, (a), non-UV treated ETPTA drops and, (b), UV treated ETPTA drops.

The observation evidencing that polymerization has occurred is the maintenance of the spherical shape during the drying process of the sample that has been irradiated with a UV torch, which tells that no coalescence has occurred, meaning that the drops are solid. On the other hand, a drop merging is observed during drying the sample which was not irradiated with UV light. At the end of the process, a single big oily drop is formed, evidencing its liquid state.

6.1.2. Colloidal crystals

Focusing now on the correctly polymerized drops system, one notable thing when observing the water evaporation is that, depending on the volume fraction corresponding to the spheres inside the water drop, a different disposition is noticed[11]. In figure 8, before starting the evaporation procedure, the spheres are disposed in an almost square distribution, whereas at the end of the evaporation process, a highly ordered hexagonal monolayer of spheres is formed with a planar packing fraction of the spheres of around 0.79. This phenomenon, which appears when the volume fraction corresponding to the particles is high[11], is not only observed in the case explained above. At the tube attached to the output of the microfluidic device, where drop accumulation can occur due to high formation rates, a hexagonal array is also observed (figure 9).

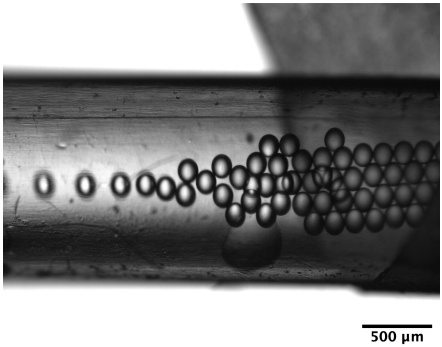

Figure 9. Hexagonal array observed at the collecting tube ($Q_{c,p}$= 65.1 µLmin^{-1} $Q_{d,p}$= 31.0 µLmin^{-1})

In addition to a high volume fraction, polymer spheres need to be highly monodisperse, not only in size but also in shape[11]. Otherwise, size fluctuations lead to the appearance of distortions in the lattice, meaning that the highly ordered spatial distribution is unachievable.

Overall, it is concluded, according to the observations above, that a colloidal crystal is formed[12]: the system is composed of a highly ordered 2D hexagonal monolayer of monodisperse colloidal spheres. So, these systems can be compared to macroscopic atoms (identically shaped and sized spheres) distributed regularly in space. And, according to this, several approaches applied to the atomic scale can be used to study these nearly macroscopic systems, such as electromagnetic radiation diffraction.

Electromagnetic radiation diffraction is a phenomenon arising from the interaction of electromagnetic waves with obstacles (objects, slits, etc.) of a size comparable to the wavelength of the radiation[13]. This behaviour can be described with the use of the Huygens principle, which states that these obstacles act as a wave generation point. In other words, when a wavefront encounters obstacles through its path, it is like if the wave was splitting into smaller units (figure 10). When the newly formed waves, interact with each other with a constructive pattern (simply, both wavefunctions combine to generate another wave resulting from its sum) or destructive pattern (a new wavefunction which results from the subtraction of the combining wavefunctions) where wavefunctions are cancelled and no light is seen. In the end, these cancellations and additions, inside a regular spatial distribution of the spheres in a plane, should lead to a diffraction pattern: bright spots where constructive interactions appear or shades where a destructive interaction takes place[13].

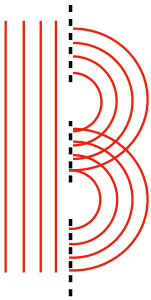

Figure 10. Schematic representation of Huygens principle, when a wave (whose wavefront is represented by the red lines) encounters two slits with a width comparable to its wavelength (obstacles). The silts act as new wavefront generating points.

To study light diffraction in the formed colloidal crystal, a monolayer of ETPTA spheres is generated through in-flow polymerization of drops created with a $Q_{d.p}$ of 94.1 µLmin^{-1} and a $Q_{c.p}$ 1.0 µLmin^{-1} (Ø=144.5 ± 0.8 µm) using device **II**. Light diffraction studies of the 2D lattice, performed with a 632.8 nm Helium-Neon laser (*Melles Griot* HeNe/5mW Laser), show a hexagonal diffraction pattern (figure 11, (a)) which is concordant with the structure observed through optical microscopy (figure 11, (b)).

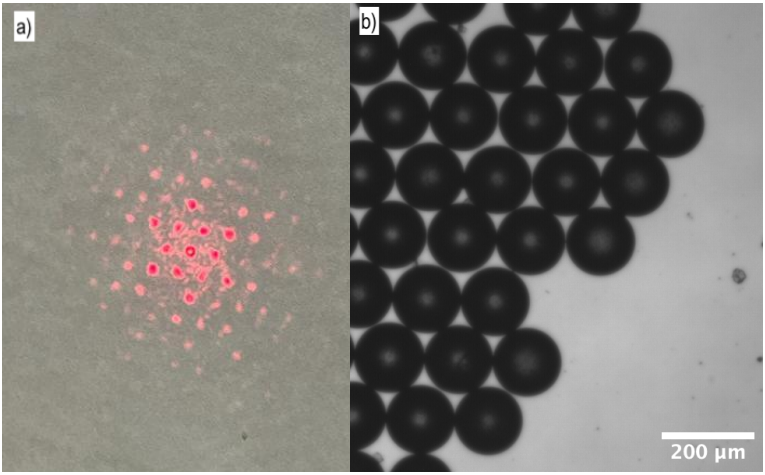

Figure 11. (a) Diffraction pattern of the colloidal crystal and, (b), the real image of the crystal.

This pattern corresponds to the reciprocal lattice of the one formed by the polymer spheres ordered as a colloidal 2D crystal. Mathematically, a reciprocal lattice can be described as the Fourier transform of a real lattice[14]. In other words, if a certain lattice can be described as a function defined by the locations[13] of each point in space, the Fourier transform of that function yields the description of its reciprocal representation. In the crystallographic world, discrete points in which spatial order can be defined with a sort of translational operations (operations which move lattice's points a certain number of unities in a certain direction), being the function that describes the system a linear combination of translational vectors[14]. Therefore, the reciprocal lattice is given by the Fourier transform of this linear combination of translational vectors. A scheme of the diffraction pattern obtained with the notation of the different dots based on Miller indexes[13], indexes used to identify unambiguously directions and planes in space, can be seen in figure 12[15–17].

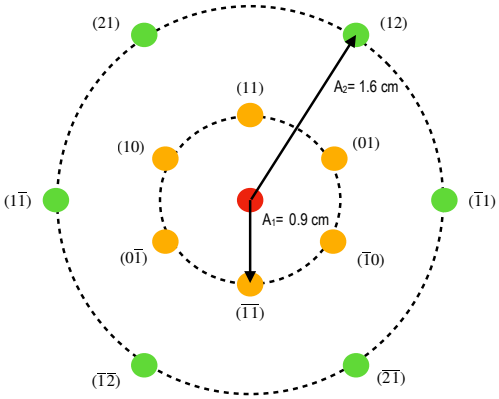

Figure 12. Scheme of the diffraction pattern obtained with the use of a red laser beam.

This reciprocal lattice has an inverse correlation with its real counterpart, meaning that when the distance between nodes or elements inside the real lattice (in the case concerned, spheres) increases, the distance between different spots is reduced in the reciprocal lattice[13].

The description of the observed pattern can be done through equation IV[18].

$$(m_1(i)^2 - m_1(i)m_2(\mathrm{i}) + m_2(i)^2)^{1/2}\lambda = \frac{\sqrt{3}}{2}\, D\, \sin\theta_i \qquad \textbf{Eq. IV}$$

Here $m_1(i)$ and $m_2(i)$ are the Miller indexes related to point i, D is the distance between spheres in the real lattice, λ is the wavelength of the electromagnetic radiation used, and θ_i is the angle of diffraction given by the experimental setup for point i, schematized at figure 13.

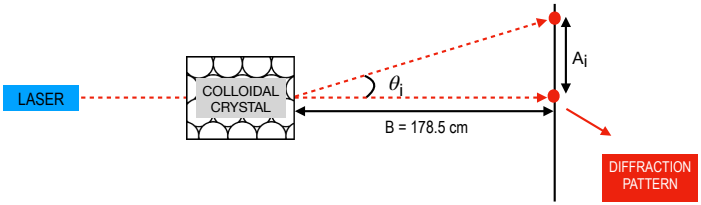

Figure 13. Scheme of the diffraction experimental setup.

As θ_i is small, its sinus can be approximated by its tangent. And thus, equation IV can be described as equation V, being $tan\ \theta_i = A_i/B$, where A_i and B are defined by the experimental setup (figure 13).

$$(m_1(i)^2 - m_1(i)m_2(\mathrm{i}) + m_2(i)^2)^{1/2}\lambda = \frac{\sqrt{3}}{2} D \frac{A_i}{B} \qquad \textbf{Eq. V}$$

The application of equation V with the use of the measurements obtained (figures 12 and 13) gives a mean inter-particle distance of 143.1 ± 1.1 μm, which is consistent with the one obtained through optical microscopy, which is 145.0 ± 1.0 μm. Therefore, this confirms that the colloidal crystal maintains its order at macroscopic distances.

6.2. FUNCTIONAL COLLOIDS

6.2.1. Silica coating and surface functionalization

To analyze applications of the generated polymer spheres, surface functionalization is explored. This section aims to generate a reactive surface that allows a wide range of functionalization possibilities. Among the best options to generate a surface with a high capacity of diverse functionalization, a silica coating over the polymer sphere has been considered, thanks to the presence of hydroxyl groups on the surface[19].

The fact that the silica-coated spheres can undergo diverse surface functionalization using silane compounds, provides a wide range of potential applications depending on the surface properties. For example, metal ions can be trapped onto spheres' surfaces through electrostatic interactions with a quaternary amine. This means that the key is proper selecting the functionalization based on the desired interactions[20]. This can lead to applications such as water

pollutants' removal, molecular targeting, or the creation of stationary phases for chromatographic techniques[19–21].

6.2.2. Liquid crystal alignment through functionalization of the silica shell

To determine whether the functionalization has occurred or not, alignment of a liquid crystal around the spheres will be studied.

A liquid crystal can be defined as a state of matter between liquid and solid. These are anisotropic liquids, i.e., liquids whose properties, such as light propagation or ionic conductivity vary as a function of the direction in which they are studied[22].

Molecules in a liquid crystal tend to align their axis in the same direction, to reduce the free energy of the system[22]. Under confinement, alignment direction (director field) can be controlled, by modelling the surface chemistry of the walls that confine the liquid crystal. Two basic dispositions can be obtained depending on this chemistry: having the molecules with their axis aligned parallelly to the surfaces' walls (planar anchoring; which is generally related when hydrophilic surfaces are present) or perpendicularly to the surfaces' walls (homeotropic anchoring; generally related to hydrophobic surfaces)[22,23].

Therefore, to analyze the functionalization of the silica-coated ETPTA spheres, a comparison between the surface anchoring conditions when having an 18 carbon saturated attached to the silica surface (using the silane DMOAP in this report, see section 7.4.2.2) or bare silica surface is assessed when the spheres are introduced inside a layer of the liquid crystal 5CB confined between two parallel glass plates that impose planar anchoring. When introducing the spheres into the system, a perturbation of the director field is expected, and its magnitude and type are a function of the anchoring characteristics on the surfaces of the spheres (figure 14)[22,23].

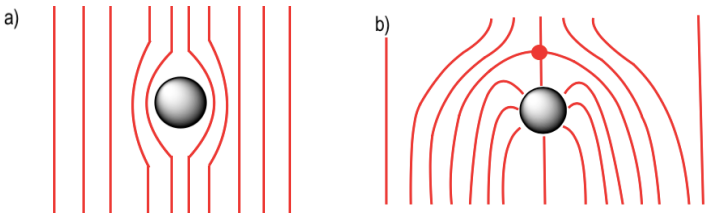

Figure 14. Director field (molecules' orientation), represented as red lines, around the polymer spheres with a bare silica surface (a), or with DMOAP surface functionalization (b).

When only silica is present over the surface, planar anchoring is expected around the sphere (the bare silica is hydrophilic), and thus, a small perturbation of the director field is expected. The field is deformed to englobe them. On the other hand, surface functionalization of the silica with DMOAP generates a stronger perturbation, as now the anchoring condition on the particle's surface is homeotropic (DMOAP is hydrophobic). As the particles are relatively big, the configuration of the director field around the sphere acquires a hyperbolic structure, because of near the surface the molecules are forced to be oriented perpendicular to it. This configuration is called hedgehog defect, and experimentally it will be observed as two bright lobes around the sphere under a polarized light microscope[23].

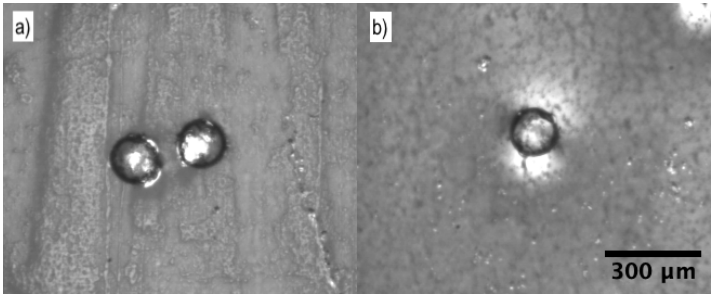

Figure 15. Polymer spheres embedded in 5-CB without, (a), or with, (b), DMOAP functionalization.

In figure 15, images acquired under the polarized light microscope of the spheres inside the liquid crystal can be seen. In these images, different values in the grayscale of the background are related to perturbations in the director field. Here, around DMOAP functionalized spheres, the presence of lighter lobes is observed, whereas non-functionalized spheres show no change in the grayscale around them. This is consistent with the distribution of the director field showed in figure 13, demonstrating that particle functionalization has been successfully accomplished.

7. EXPERIMENTAL SECTION

7.1. DROP OBSERVATION AND DATA ANALYSIS

The study of the drops generated, and characterization of the devices are performed with the use of an optical microscope (*Euromex Oxion Inverso*) and a polarized light optical microscope (*Nikon Eclipse 50iPOL*). The images are collected with cameras attached to the microscopes (*ThorLabs and Marlin-Allied Vision Technologies*). Image processing and data analysis were performed with the use of *ImageJ*, *Microsoft Excel,* and *Matlab* softwares.

7.2. DROP-GENERATOR MICROFLUIDIC DEVICES

7.2.1. Materials used

For the construction of the needle-based device's combination of 22 gauge (22G) and 27 gauge (27G), and 30 gauge (30G) and 34 gauge (34G), blunt tip steel needles are used (*Like Sun GmbH*). The outer structure of the device is made of a polyethylene T-junction (2.3 cm × 1.4 cm-inner Ø=8 mm). The overall support is composed of a glass slide (*Duran Wheaton Kimble*).

In the case of glass-based devices, the inner glass capillaries are made of borosilicate (inner Ø=0.5 mm-outer Ø=0.8 mm-*WPI*) and the outer structure where the smaller glass capillaries are inserted is composed of a round borosilicate capillary (inner Ø=1.2 mm-outer Ø=1.9 mm-*WPI*). The overall support is composed of two glass slides (7.5 cm × 5.2 cm-*Scientific Glass Laboratories ltd.).*

The structures are fixed with the use of fast setting epoxy glue (*Devcon*). To characterize the system in terms of architecture, the inner diameters (Ø) of the inlets and outlets and the inter-tips distance of each device are used. Inner diameters in the case of needle-based devices are given by the gauge used. In the case of glass-based devices, to determine inner diameters of the tips working as outlets and inlets, as well as the distance between these tips, an optical microscope (*Euromex Oxion Inverso*) is used. To better understand the whole structure of the

different devices, a scheme of a needle and glass-based device is seen in appendix 2, figure B.1 and appendix 3, figure C.1, respectively.

7.2.2. Construction of needle-based devices

7.2.2.1. General construction procedure

The following steps, based on Li T. et al. procedure[8], are performed to build a needle-based drop-generator device based on flow-focusing:

1.- First, plastic adapter of the collector needle is removed with the help of a heater gun. This is done to have a proper exit of drops at the end of the collector needle, otherwise, drops can accumulate inside the plastic adapter and fuse.

2.- About half of a centimetre of one end of the T-Junction plastic piece is removed in order to fit the needles properly (see appendix 2, figure B.2).

3.- All the pieces are cleaned at the same time. First, a washing with ethanol (95% vol.) is performed inside an ultrasound bath for 15 min. Afterwards, the pieces are washed again inside an ultrasound bath for 15 min, changing the ethanol with Milli-Q water. Then, everything is properly dried under an N_2 flux.

4.- On a glass slide, the T-junction plastic piece is fixed with the help of fast setting epoxy glue (see appendix 2, figure B.3). Once it is fixed, the outlet needle is attached to the non-cut end of the plastic piece using fast setting epoxy. The needle should be as far from the centre of the piece as possible but without being just at the edge. The needle should be properly centred inside the tube to acquire a good performance when forming the drops. This centring is carried out using an optical microscope (see appendix 2, figure B.4).

5.- The dispersed phase inlet needle is attached to the device with fast setting epoxy resin. It needs to be coaxial to the outlet needle. The microscope is used to centre the inlet needle. The device should rest for at least one hour before use to avoid epoxy cracking because of liquids' pressure when pumping the phases (see appendix 2, figure B.5).

6.- With the use of needle-tip adapters to couple the needles to a flexible tube, and flexible tube connections, the inlets are connected. A tube is glued to the outlet needle to better control drop collection and observation. The continuous phase enters from the perpendicular orifice of the plastic device. An image of the device can be seen in appendix 2, figure B.6.

Following this procedure, several devices are constructed. The parameters that characterise the construction and the devices built are shown in table II.

Device	Combination type	Dispersed phase inlet needle Ø [μm][8]	Outlet needle Ø [μm][8]	Inter-needle tips distance [μm]
I	30G+34G	60 ± 10	160 ± 10	403.80 ± 0.02
II	30G+34G	60 ± 10	160 ± 10	105.62 ± 0.02
III	22G+27G	210 ± 10	410 ± 10	592.12 ± 0.02

Table II. Non-surface-functionalized needle-based device characterization parameters.

7.2.2.2. Surface functionalization of needles

To build a hydrophobic device to prepare W/O emulsions, all plastic caps are removed in step 1, and a functionalization step is added, consisting of submerging the needles inside a 3% wt. solution of OTS (90%-*Aldrich*) in toluene (99.8%-*ABCR*) for 30 min. After the functionalizing bath, the needles are flushed with an N_2 stream and cured thermally at 80ºC for 1h.

The parameters associated with the device constructed with needle functionalisation are shown in table III.

Device	Combination type	Dispersed phase inlet needle Ø [μm][8]	Outlet needle Ø [μm][8]	Inter-needle tips distance [μm]
IV	22G+27G	210 ± 10	410 ± 10	471.90 ± 0.02

Table III. Surface functionalized needle-based device characterization parameters.

7.2.3. Construction of glass-based devices

The following steps, based on Guerrero J. et al. procedure[9], are performed, to build a glass-based drop-generator device with flow-focusing configuration:

1.- To create the dispersed phase capillary and the collector capillary, a borosilicate capillary is pulled with a laser capillary pulling machine (*Sutter*). After the pulling is performed, the capillary stretched tips are cut with the use of a microforge (*Narishige*) to the desired diameter. The optimized diameters' relation to performing droplet formation[9] is that the bigger diameter is twice the size that of the smaller ones.

2.- The two inner glass capillaries and the outer round glass capillary are cleaned with sulphochromic mixture and rinsed with Milli-Q water. All the capillaries are dried under an N_2 flux after cleaning.

3.- A glass plate is prepared by attaching two glass slides with epoxy resin two small glass pieces (see appendix 3, figure C.2).

4.- The inlet and outlet needles are prepared from 19G needles (*Terumo*). The sharp tips of 19G needles are cut with the use of a radial saw. Then, the plastic adapters of the needles are cut to let the capillaries fit through. Then, the needles are washed with Milli-Q water in an ultrasound bath and dried under an N_2 flux afterwards.

5.- The outer round capillary is fixed with fast setting epoxy resin onto the glass plate (see appendix 3, figure C.3). Once the resin is hard enough to not move the round capillary, the inlet and collector capillaries are inserted inside the fixed capillary and adjusted to their correct position. Ideally, the distance between the glass tips should be similar to the diameter of the dispersed phase inlet tip diameter. The setup is fixed with fast setting epoxy (see appendix 3, figure C.4).

6.- The inlet and outlet needles are fixed to their position with fast setting epoxy. The resin must be viscous enough to avoid infiltrations inside the device. Therefore, the glue must be applied from 5 to 8 minutes after the effective mixture of the two epoxy resin components (see appendix 3, figure C.5).

7.- The device is sealed with more epoxy and let to rest for 10h before use, to avoid epoxy cracking. Then the device is connected to the pumping system with flexible tubes. An image of the device can be seen in appendix 3, figure C.6.

The parameters which characterize the constructed glass-based device are seen in table IV.

Device	Dispersed phase inlet capillary tip Ø [µm]	Outlet capillary tip Ø [µm]	Inter-tips distance [µm]
V	38.92 ± 0.02	68.28 ± 0.02	89.32 ± 0.02

Table IV. Glass-based device characterization parameters.

7.3. DROP GENERATION

7.3.1. Pumping system and drop collection

The liquids are pumped through the device with the use of syringe pumps (*WPI*). The connection between the pumps and the device inlets is accomplished with the use of fine bore polyethylene tubes (inner Ø= 0.86 mm-outer Ø= 1.52 mm-*Smiths Medical International Ltd.*). Before entering the system, continuous and dispersed phases are filtered with 0.2 µm

polytetrafluoroethylene filters (*Acrodisc*). Drops are collected in a PDMS device in the case of hexadecane oil drops (to have a better observation of them) which is connected to the outlet of the drop-generator device through polyethylene tubes.

7.3.2. Dispersed and continuous phases

The continuous phase used in every experiment is a 2.03% wt. solution of surfactant F-127 (also known as Pluronic acid) in water. To prepare 50.077 g of solution, 1.019 g of F-127 (*Sigma*) are combined with 49.058 g of Milli-Q water[8]. The resultant mixture is stirred at room temperature for 30 min and then, sonicated for 15 min.

Hexadecane oil (99%-*Sigma-Aldrich*) is directly used as a dispersed phase in some experiments.

To generate polymer spheres, the solution consisting of a 1.39% wt. mixture HMPP photoinitiator in ETPTA monomer is used as the dispersed phase[8]. 21.207 g of the mixture are prepared by combining 0.299 g of HMPP (97%-*Sigma-Aldrich*) and 21.207 g of EPTA monomer (*Sigma-Aldrich*). To ensure proper mixing, the solution is stirred for 1h at room temperature. As the mixture is sensitive to light, the recipient is covered with aluminium foil.

7.4. POLYMER SPHERES

7.4.1. Polymerization procedure

To polymerize the drops, an UV light torch (*Alonefire*-365nm/5W) is used in different regimes: in-flow polymerization and after collecting polymerization.

For after-collecting polymerization, the drops are generated and collected directly from the device. Then, the collected drops are polymerized applying UV light for 30 seconds.

For in-flow polymerization, a UV chamber is built with the use of a homemade expanded polystyrene structure, aluminium foil, and polyethylene tubes. The UV torch is inserted from the top and the connection to the drop-generator device is accomplished through a flexible silicon transparent flexible tube (inner Ø=1.6 mm). Polymerization occurs while the drops are flowing through the tubes.

7.4.2. Silica coating and surface functionalization of the spheres

7.4.2.1. Silica coating

A general procedure to create a thin layer of SiO_2 over diverse types of particles is the one described by Graf C. et al. [24]. In the first step, a solution of PVP (MW=360.000 $gmol^{-1}$-*Sigma*) is prepared by adding 1 mg of the polymer to 4 mL of MilliQ-water to have more than 60 molecules of PVP for each nm^2 of surface to cover. To the solution of PVP, the particles are added, and the resultant mixture is vortex-stirred for 24h. After the stirring process, the supernatant is removed, and 5 mL of a solution (4.9% v/v) composed of NH_3 (29%-*Sigma-Aldrich*) in ethanol (96% v/v) is added. Then, the new solution is stirred and 100 µL (10% wt.) of TES (99%-*Aldrich*) in ethanol (96% vol.) is introduced dropwise while stirring. The final system is vortex-stirred for 24h. Finally, the particles are removed from the mixture and cleaned with Milli-Q water and stored in a water-ethanol mixture (1:1).

7.4.2.2. Surface functionalization

The coated polymer spheres are functionalized with DMOAP as it is described in Pagès, J.M. [25]. In 4 mL of Milli-Q water, 33 µL of DMOAP (60% v/v sol. in methanol-*Acros Organics*) is added. To ensure proper mixing of both liquids, the solution is sonicated for 15 minutes. The silica-coated ETPTA spheres are added to the mixture. The system is vortex-stirred for 30 min. Once, the agitation is completed, the supernatant is removed, and the spheres are cleaned with Milli-Q water and stored in a water-ethanol mixture (1:1).

7.4.3. Liquid crystal cells

To prepare a liquid crystal cell, a glass slide is cut to extract two 2 cm × 2.5 cm pieces. These pieces are washed first with soap and distilled water and then sonicated for 15 min inside a Milli-Q water-surfactant *(DECON90®)* mixture. Once, the surface is cleaned, it is activated by submerging the glass pieces inside sulphochromic mixture for 1 min each. Then, the glasses are coated with 826 polyimide (*Nissan*) by using the spin-coating technique and thermally treated (80ºC (5min)- 280ºC(1h)). Once the pieces are prepared, the surface is rubbed with a soft fabric, and the cell is built putting the glass pieces one over the other, using nylon wire as the spacer (Ø=0.22 µm-*Smart SLR*). The structure is fixed with the use of epoxy resin (*Devcon*). Observation is made with the use of a polarized light optical microscope (*Nikon Eclipse 50iPOL*) and images recording using a camera attached to it (*Marlin-Allied Vision Technologies*).

8. CONCLUSIONS

Needle-based devices can be inexpensive candidates to substitute glass-based devices to obtain monodisperse emulsions, as it is shown in this report. With the use of flow-focusing as the method used to perform the generation of monodisperse drops, the parameters which regulate the performance of the devices, and thus, the monodispersity and size of the drops, have been remarked, showing the importance of the architecture of the system in addition to the flow rates of the liquid phases. Moreover, a comparison in terms of construction difficulty, risks, and performance of different material-based microfluidics is provided, making emphasis on the possibility of applying the technique inside a master's or undergraduate academic laboratory, to introduce microfluidics to students.

As an application of drop-generator microfluidic devices, ETPTA polymer monodisperse spheres have been generated, showing the capability of the technique to generate colloidal materials. It has been observed that monodisperse (in size and shape) monolayers of spheres tend to arrange in a hexagonal packing forming a colloidal crystal, and light diffraction studies can be performed to demonstrate this disposition, in addition to microscope observations. This suggests the possibility of using this microparticles to build diffraction gratins or other photonic devices.

To further explore of the possibilities that polymer spheres could provide, functionalization of their surface is performed through generating a silica shell followed by a silane functionalization. This demonstrates that surface properties can be tuned, and several applications arise according to this possibility, such as pollutant removal from waters.

9. REFERENCES AND NOTES

1. Elvira, K. S., Gielen, F., Tsai, S. S. H. & Nightingale, A. M. Materials and methods for droplet microfluidic device fabrication. *Lab on a Chip,* **2022,** 22, 859–875.
2. Whitesides, G. M. The origins and the future of microfluidics. *Nature,* **2006**, 442, 368–373.
3. Zhu, P. & Wang, L. Passive and active droplet generation with microfluidics: a review. *Lab on a Chip,* **2017**, 17, 34–75.
4. Shang, L., Cheng, Y. & Zhao, Y. Emerging Droplet Microfluidics. *Chemical Reviews,* **2017**, 117, 7964–8040.
5. Lian, Z. et al. Microfluidic formation of highly monodispersed multiple cored droplets using needle-based system in parallel mode. *Electrophoresis,* **2020**, 41, 891–901.
6. Chappat, M. Some applications of emulsions. *A: Physicochemical and Engineering Aspects,* **1994**, 91, 55-57.
7. Park, S. H., Hong, C. R. & Choi, S. J. Prevention of Ostwald ripening in orange oil emulsions: Impact of surfactant type and Ostwald ripening inhibitor type. *LWT,* **2020**, 134, 110180.
8. Li, T., Zhao, L., Liu, W., Xu, J. & Wang, J. Simple and reusable off-the-shelf microfluidic devices for the versatile generation of droplets. *Lab on a Chip,* **2016**, 16, 4718–4724 (2016).
9. Guerrero, J., Rojo, J., de la Cotte, A., Aguilera-Sáez, J.M., Vila E. & Fernandez-Nieves, A. Glass-Based Devices to Generate Drops and Emulsions. *Journal of Visualized Experiments,* **2022**, 182, 1-20.
10. Jin, S. H., Kim, T., Oh, D., Kang, K. K. & Lee, C. S. Preparation of monodisperse PEGDA microparticles using a dispensing needle based microfluidic device. *Korean Chemical Engineering Research*, **2019**, 57, 58–64.
11. Shui, L., Stefan Kooij, E., Wijnperlé, D., van den Berg, A. & Eijkel, J. C. T. Liquid crystallography: 3D microdroplet arrangements using microfluidics. *Soft Matter*, **2019**, 5, 2708–2712.
12. Okubo, T. POLYMER COLLOIDAL CRYSTALS. *Progress in Polymer Science*, **1993**, 18, 481-517.
13. Hammond, C. Crystallography and Diffraction. *Oxford Science Publications*, 3rd Edition, **2009**, 131-181.
14. Krowne, C. M. Determination of reciprocal lattice from direct space in 3D and 2D - Examination of hexagonal band structure. *Advances in Imaging and Electron Physics,* **2019**, 210, 7–22.
15. Romanov, S. G. Light diffraction features in an ordered monolayer of spheres. *Physics of the Solid State*, **2017**, 59, 1356–1367.
16. Samusev, A. K. et al. Two-dimensional light diffraction from thin opal films. *Physics of the Solid State,* **2011**, 53, 1056–1061.
17. Dux, C. & Versmold, H. Light Diffraction from Shear Ordered Colloidal Dispersions. *Physical Review Letters*, **1997**, 79, 1811-1814.
18. Krieger, I.M., O'Neill, F.Diffraction of Light by Arrays of Colloids. *Journal of the American Chemical Society,* **1968**, 90, 3114-3120.
19. Wu, Z. et al. Controlling the hydrophobicity of submicrometer silica spheres via surface modification for nanocomposite applications. *Langmuir*, **2007**, 23, 7799–7803.
20. Wieszczycka, K., Staszak, K., Wozniak-Budych, M.J., Litowczenko, J., Maciejewska B.M. & Jurga, S. Surface functionalization – The way for advanced applications of smart materials. *Coordination Chemistry Reviews*, **2021**, 436, 213846.

21. Akhavan, B., Jarvis, K. & Majewski, P. Tuning the hydrophobicity of plasma polymer coated silica particles. *Powder Technology*, **2013**, 249, 403–411.
22. Muševič, I., Škarabot, M., Tkalec, U., Ravnik, M. & Žumer, S. Two-dimensional nematic colloidal crystals self-assembled by topological defects. *Science*, **2006**, 313, 954–958.
23. Hirankittiwong, P. et al. Optical manipulation of the nematic director field around microspheres covered with an azo-dendrimer monolayer. *Optics Express*, **2014**, 22, 20087.
24. Graf, C., Vossen, D. L. J., Imhof, A. & van Blaaderen, A. A general method to coat colloidal particles with silica. *Langmuir*, **2003**, 19, 6693–6700.
25. Pagès, J.M.. Transport and assembly of colloids in liquid crystals. *Universitat de Barcelona*, **2019**, 72.
26. Vijayakumar, V., Anothumakkool, B., Kurungot, S., Winter, M. & Nair, J. R. In situ polymerization process: An essential design tool for lithium polymer batteries. *Energy and Environmental Science*, **2021**, 14, 2708–2788.
27. Kalybekkyzy, S., Kopzhassar, A. F., Kahraman, M. V., Mentbayeva, A. & Bakenov, Z. Fabrication of uv-crosslinked flexible solid polymer electrolyte with PDMS for li-ion batteries. *Polymers (Basel)*, **2021**, 23, 1–12.
28. United Nations, Department of Economic and Social Affairs: Sustainable development, *https://sdgs.un.org*. Accessed 26th of May, **2022**.

10. ACRONYMS

CV: Coefficient of variation.

ETPTA: Trimethylolpropane ethoxylate triacrylate.

DMOAP: Dimethylocatadecyl[3-(trimethoxysilyl)propyl)ammonium chloride.

HMPP: 2-Hydroxy-2-methylpropiophenone.

MW: Molecular weight.

OTS: N-Octadecyltrichlorosilane.

PDMS: Polydimethylsiloxane.

PVP: Polyvinylpyrrolidone.

TES: Tetraethoxysilane.

UV: Ultraviolet.

W/O: Water-in-oil.

O/W: Oil-in-water.

5CB: 4'-Pentyl-4-biphenylcarbonitrile.

2D: bidimensional.

3D: tridimensional.

.

APPENDICES

APPENDIX 1: POLYMERIZATION MECHANISM

The polymerization mechanism of ETPTA occurring inside the drops generated with the use of microfluidics is promoted by the action of UV light[26,27]. The description of the mechanism is based on the fact that the main reactivity explaining the process is due to the presence of vinyl groups in the monomer. In figure A, the structure of the monomer is seen.

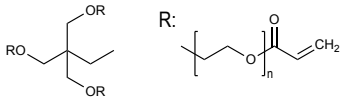

Figure A. ETPTA structure.

The reaction is started through the photolysis of the initiator. The initiator, HMPP, which is located inside the drop, splits under UV irradiation into free radicals. The breaking procedure is seen in the scheme I[25]. These radicals are reactive species that attack the vinyl group of ETPTA monomers provoking the activation of the molecules.

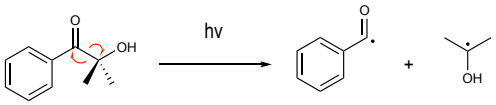

Scheme I. HMPP light breakage.

To simplify the explanation of the polymerization process, a general vinyl group is considered, which can be related to ETPTA as the fragment represents. In scheme II, the vinyl group activation by a radical **I** is observed[26]. It is seen that the free electron of the radical attacks the double bond of the group, generating another one, which is regarded as an activated specie.

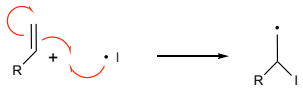

Scheme II. Initiation step.

The propagation of the structure occurs via a radical attack of the activated species generated (radicals). In scheme III[25], the propagation of the chain occurs. This procedure reassembles a chain reaction mechanism because the reaction promoted by an activated species yields another activated specie.

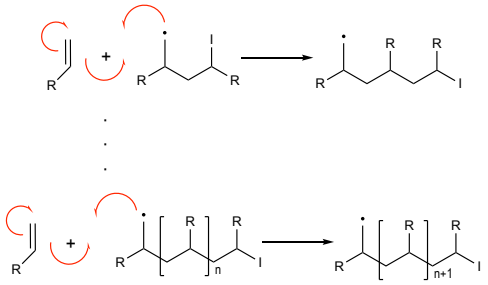

Scheme III. Propagation steps.

The mechanism is ended when the deactivation of the active species occurs. This deactivation appears when two active species (radicals) react in a single step to yield the formation of an inactive structure without radicals. The procedure can occur via two processes seen in scheme IV[26]. In the ETPTA polymerization process, recombination (1) is favoured over disproportionation (2).

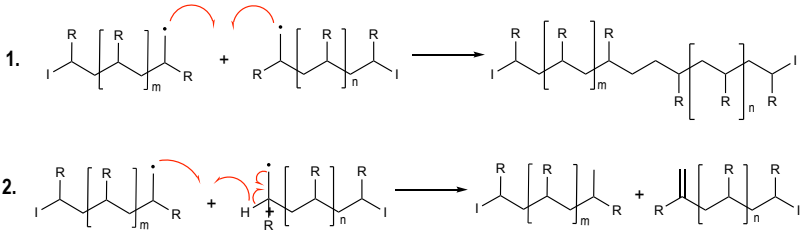

Scheme IV. Termination steps.

As ETPTA is a monomer with three vinyl groups, each group follows the pattern shown above. Provided that each molecule of ETPTA can react in three different areas, a 3D structure is acquired at the end of the polymerization process, yielding a cross-linked polymer[27].

APPENDIX 2: SCHEMES FOR THE NEEDLE-BASED DEVICE

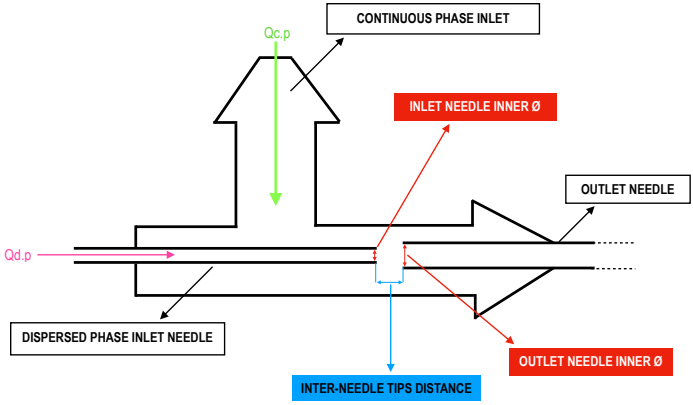

Figure B.1. System's scheme with characterization parameters.

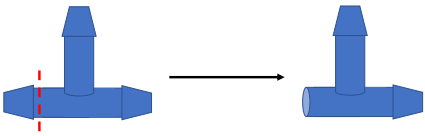

Figure B.2. T-junction cutting.

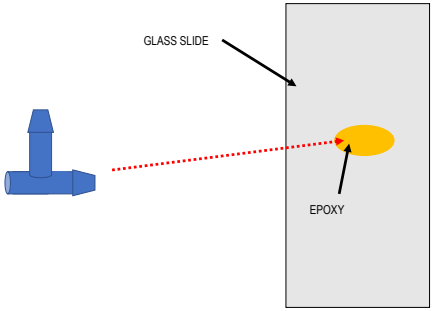

Figure B.3. T-junction assembling.

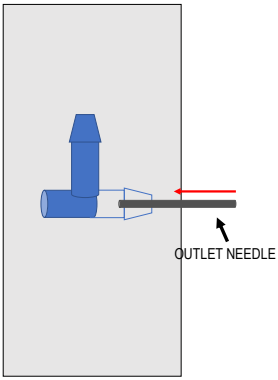

Figure B.4. Outlet needle assembling.

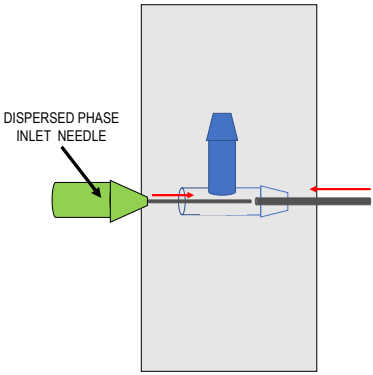

Figure B.5. Inlet needle assembling.

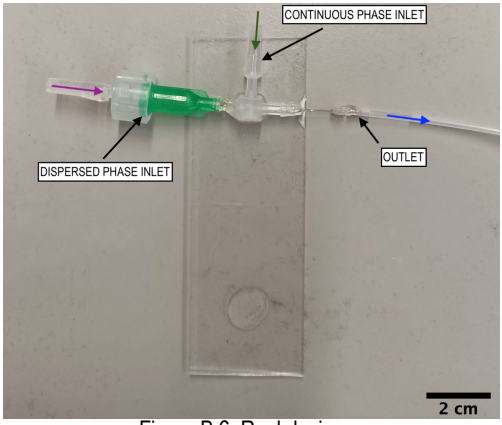

Figure B.6. Real device.

APPENDIX 3: SCHEMES FOR THE GLASS-BASED DEVICE

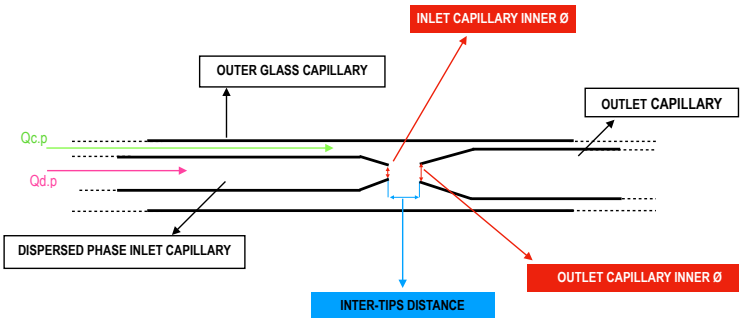

Figure C.1. System's scheme with characterization parameters.

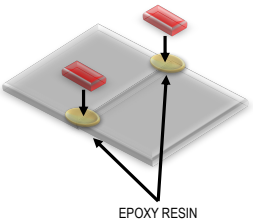

Figure C.2 Base construction.

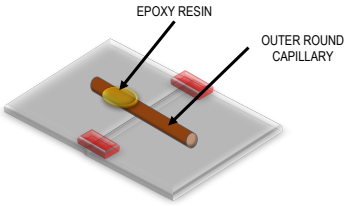

Figure C.3. Outer capillary assembling.

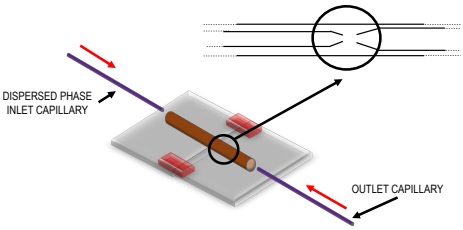

Figure C.4. Inlet and outlet capillaries assembling.

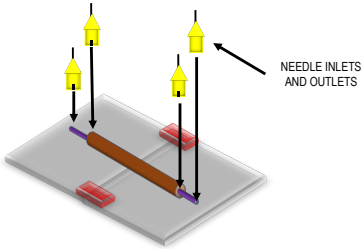

Figure C.5. Needle inlets and outlets assembling.

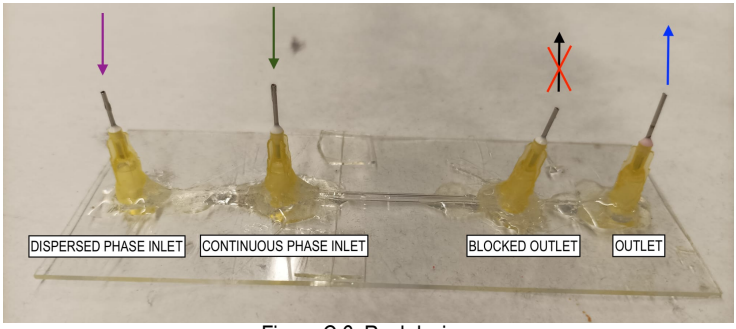

Figure C.6. Real device.